Nuclide production cross section of ^{nat}Lu target irradiated with 0.4-, 1.3-, 2.2-, and 3.0-GeV protons

Hayato TAKESHITA[1,2], Shin-ichiro MEIGO[2], Hiroki MATSUDA[2], Hiroki IWAMOTO[2],

Keita NAKANO[2], Yukinobu WATANABE[1], Fujio MAEKAWA[2]

[1]Department of Advanced Energy Engineering Science, Kyushu University

[2]J-PARC Center, Japan Atomic Energy Agency

email: takeshita.hayato.890@s.kyushu-u.ac.jp

Proton-induced nuclide production cross sections of ^{nat}Lu target were measured at incident energies of 0.4, 1.3, 2.2, and 3.0 GeV by means of the conventional activation method. The targets were irradiated by the proton beam generated from the 3 GeV Rapid Cycling Synchrotron of Japan Proton Accelerator Research Complex. Gamma-rays emitted by the irradiated samples were detected by two high purity Ge detectors. The experimental data were compared with model predictions to benchmark reaction models used in the simulation of particle transport in matter, INCL4.6/GEM and INCL++/ABLA07.

1. Introduction

For the design of high-energy accelerator facilities such as accelerator-driven transmutation systems (ADSs) and spallation neutron sources, reliable assessment of radioactivity in target and structural materials requires sufficiently accurate estimation of the production yields of radioactive nuclides. Although a great deal of effort has been devoted to studying the spallation reactions from both the theoretical and experimental [1, 2] perspectives, the prediction powers of theoretical models are still insufficient. As for the experiments, relatively large uncertainties (~10%) in the experimental data make it difficult to improve the theoretical models. To obtain accurate experimental data required for improving the theoretical models, we have conducted a series of systematic measurements of nuclide production cross sections for various targets using the 3 GeV Rapid Cycling Synchrotron (RCS) accelerator at the Japan Proton Accelerator Research Complex (J-PARC). Our previous experiments for Al, Pb, and Bi targets [3,4] showed that a well-calibrated current transformer successfully reduced the uncertainty in the beam current, which finally achieved approximately 3.6% as the minimum total uncertainty.

To improve theoretical reaction models, further experimental data are required in the GeV range where the experimental data are insufficient. Recently, we have measured the nuclide production cross sections for Ho, Lu, and Re at 0.4, 1.3, 2.2, and 3.0 GeV to meet the requirement. In this paper, we show preliminary results of ^{nat}Lu. In addition, we compare the measured data with theoretical model calculations using INCL4.6/GEM [5, 6] and INCL++/ABLA07 [7, 8].

2. Experiment

The sample foils were assembled in four stacks as shown in Figure1. In each stack, Ho, Lu, and Re targets

were put in order of increasing atomic number. To prevent the products from escaping to the other target, Al foils were inserted between samples. All foils were 25 mm × 25 mm square and 0.1-mm thick. Four sets of stacks were enclosed in 0.1-mm-thick Al containers, and were fixed on movable stages in a vacuum chamber, which was installed in the beam dump line. Each stack was inserted to the irradiation position, and irradiated by proton beam with energies of 0.4, 1.3, 2.2, and 3.0 GeV. The beam profiles and currents were monitored by multi-wire profile monitors [9] installed in the beam transport line. Typical irradiation time was approximately 100 seconds.

After the irradiation, gamma-ray measurement was performed with two high-purity Ge detectors. Energy calibration and determination of detection efficiency of the detectors were performed with standard gamma-ray sources ^{137}Cs, ^{60}Co, ^{152}Eu, and ^{241}Am. The gamma-ray measurement was periodically performed with different intervals ranging from 0.5 hours to 7 days. During the measurement, an acrylic spacer was placed between the sample and the detector to keep the geometrical detection efficiency constant.
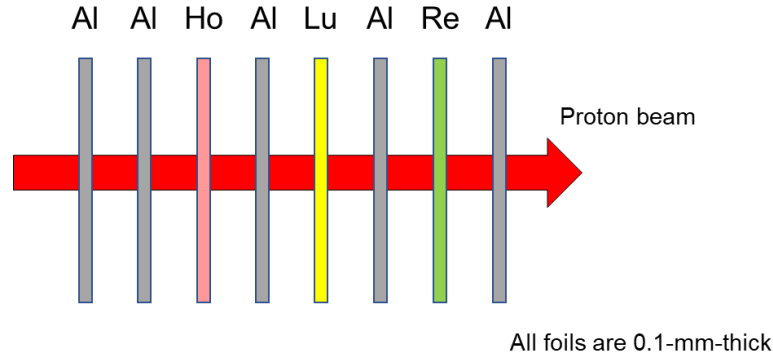
Figure 1. Schematic drawing of a sample stack.

3. Data Analysis

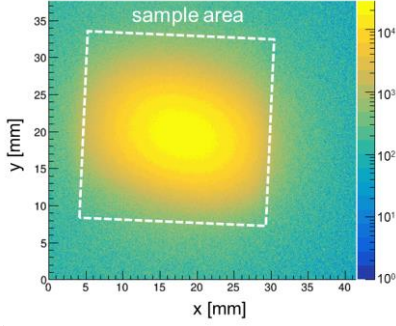### 3.1 Determination of the number of protons

During the experiment, the total number of protons irradiated to the samples was monitored by the multi-wire profile monitors. However, a part of protons transits without bombarding the sample because of the spatial expanse of the proton beam. To determine accurately the number of protons that bombarded the sample foils, two-dimensional activation distributions of the foils were taken by the FUJIFILM BAS-SR2040 imaging plate. Here, we assumed that the activation distribution is identical to the proton-beam profile. Figure 2 shows an example of the activation distributions of Lu target irradiated by 3.0-GeV protons. The proton-beam profile is well approximated by the two-dimensional gaussian:

$$f(x,y) = \frac{N}{2\pi\sigma_x\sigma_y\sqrt{1-\rho^2}}\exp\left[-\frac{1}{2(1-\rho^2)}\left\{\frac{(x-\mu_x)^2}{\sigma_x^2} + \frac{(y-\mu_y)^2}{\sigma_y^2} - \frac{2\rho(x-\mu_x)(y-\mu_y)}{\sigma_x\sigma_y}\right\}\right], \quad (1)$$

where N, μ_x, μ_y, σ_x, σ_y, and ρ are the fitting parameters. By fitting the activation distribution, the number of protons that bombarded the sample, N_{proton}, were determined by

$$N_{proton} = N_{total\ proton} \times \frac{1}{N}\int_{foil} f(x,y)dxdy, \quad (2)$$

where $N_{total\ proton} = 2.30 \times 10^{14}$ was measured by the current transformer. For this correction, typical correction factor, $N_{proton}/N_{total\ proton}$ was approximately 0.97.

Figure 2. Example of activation distribution taken by an imaging plate

Table 1. Number of protons bombarding the sample

Proton energy [GeV]	N_{proton}
0.4	2.17×10^{14}
1.3	2.26×10^{14}
2.2	2.26×10^{14}
3.0	2.23×10^{14}

3.2 Cross section determination

Figure 3 shows an example of the gamma-ray spectrum for 3.0-GeV proton irradiation. The number of products at time t after proton irradiation was obtained by

$$N_{product}(t) = \frac{C(t, t_m)}{(1 - e^{-\lambda t_m}) I_\gamma \varepsilon_p}, \tag{3}$$

where $C(t, t_m)$ is the number of peak counts in a gamma line with the measurement time t_m, λ is the decay constant of the product nuclide, I_γ is the gamma intensity, and ε_p is the peak efficiency of the detector. Figure 4 shows some examples of decay curves obtained for ^{24}Na and ^{172}Lu. The fitting curve is expressed by

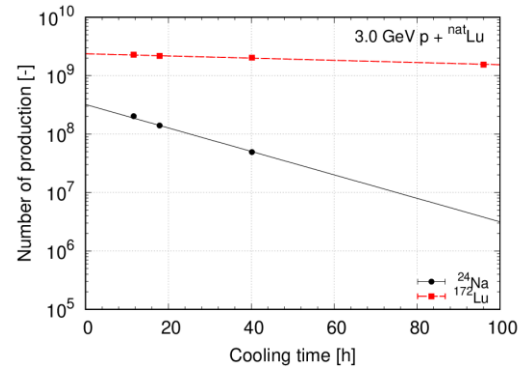$$N_{product}(t) = N_{product}(t = 0) e^{-\lambda t}, \tag{4}$$

where the number of products at the end of proton irradiation, $N_{product}(t = 0)$, was determined as a fitting parameter. Finally, the production cross section σ was obtained by

$$\sigma = \frac{N_{product}(t = 0)}{n N_{proton}}, \tag{5}$$

where n is the areal number density of target nuclei in the sample foil.
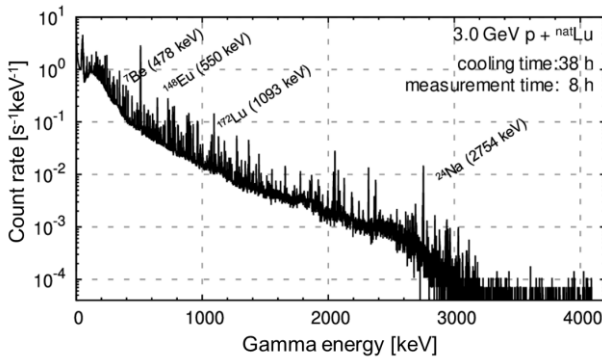
Figure 3. Example of gamma-ray spectrum

Figure 4. Example of decay curve fitting

3.3 Correction for incoming and escape of reaction products

In the sample stack, Al foils were inserted to prevent the reaction products in the sample foil from escaping to the other sample foils. However, light reaction products generated in the Al foil and other sample foils such as [7]Be, [22]Na, and [24]Na may escape to the neighboring foils. In this work, the contribution of product escape was corrected on the basis of the simulation by Particle and Heavy Ion Transport code System (PHITS) [10]. All input parameters were set to default values. For proton-induced reaction, the INCL4.6/GEM model was used. Particle transport of the reaction products including [7]Be, [22]Na, and [24]Na was simulated by using the same sample stack geometry as in the measurement. The simulation tallied the total number of the products of interest generated in the Lu foil (N_{pro}) and the number of reaction products which finally stopped in the Lu foil by ion transport among the reaction products generated in the Lu and neighboring Al foils (N_{stop}). The latter number N_{stop} corresponds to $N_{product}(t = 0)$ in Eq.(5). The correction factor for the Lu foil was defined as $N_{corr} = N_{pro}/N_{stop}$. In this work, the correction was applied only for the [7]Be production. It should be noted that the corrections for [22]Na and [24]Na heavier than [7]Be were negligibly small (less than 1%).

Table 2. Correction factors for [7]Be produced in the Lu target

| Proton energy [GeV]	N_{corr}
0.4	0.52
1.3	0.80
2.2	0.97
3.0	0.99

4. Results and Discussion

4.1 Comparison with model predictions

Figure 5 shows the production cross sections of [7]Be, [24]Na, [148]Eu, and [172]Lu. In the figure, the previous data [11] are also plotted. The production cross sections of light nuclides, e.g. [7]Be and [24]Na, increase with increasing incident proton energy. This could be because the residual nuclei generated after INC process have higher excitation energy with increasing incident energy and are likely to emit nucleons and light ions including [7]Be in the subsequent evaporation processes. The INCL4.6/GEM calculation generally reproduced the energy dependence of the cross sections except for [24]Na. The INCL++/ABLA07 calculation showed good agreement with the experimental values for [24]Na, [148]Eu, and [172]Lu. Both the two model calculations underestimated the production cross section of [7]Be.

5. Summary and outlook

Nuclide production cross sections of [nat]Lu were measured by irradiation of 0.4, 1.3, 2.2, and 3.0-GeV protons at J-PARC. In the report, we showed preliminary results of production cross sections for [7]Be, [24]Na, [148]Eu, and [172]Lu. The present data is very useful for model improvement, because the cross section data of Lu target is very limited. To investigate the prediction power of the above-mentioned models for [7]Be production, [7]Be production
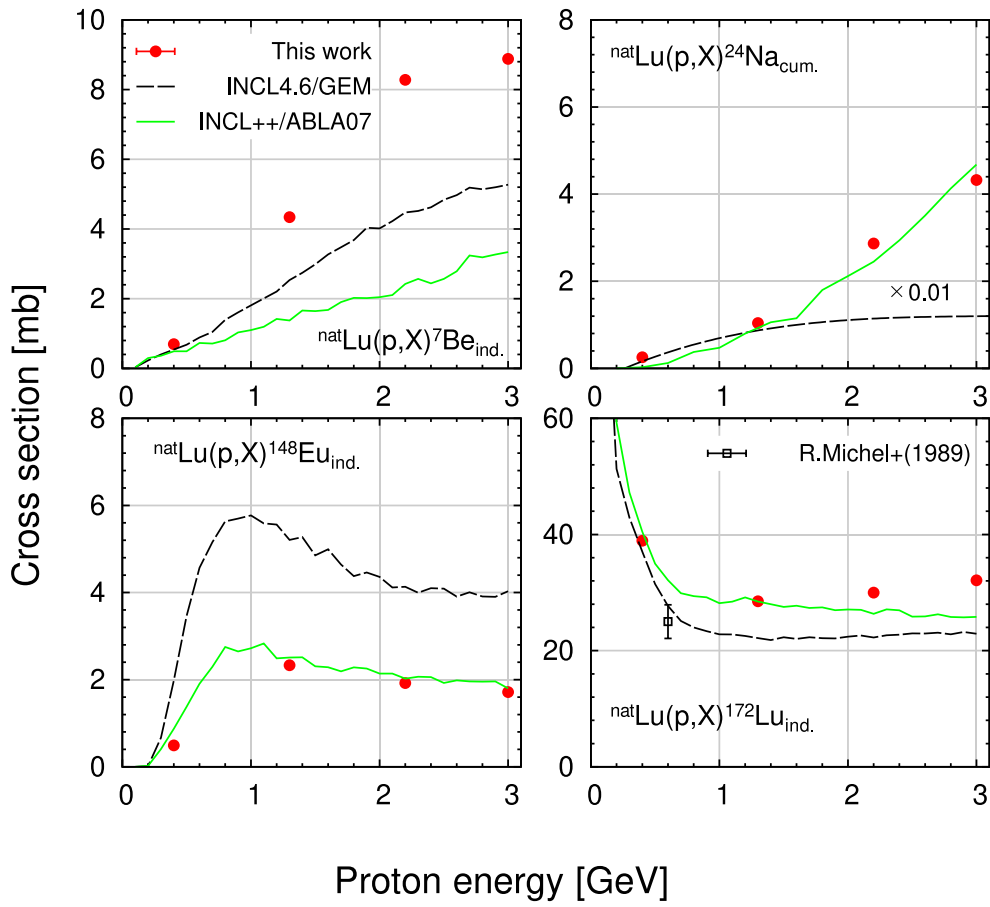
Figure 5. Experimental production cross sections for ^{7}Be, ^{24}Na, ^{148}Eu, ^{172}Lu produced by p + ^{nat}Lu reaction and model predictions by INCL4.6/GEM and INCL++/ABLA07. The subscripts ind. and cum. represent independent and cumulative cross sections. The experimental data were taken from [11]. The calculation results for ^{24}Na by the INCL4.6/GEM calculation was multiplied by 100. Our data shows statistical uncertainties, but included in the maker.
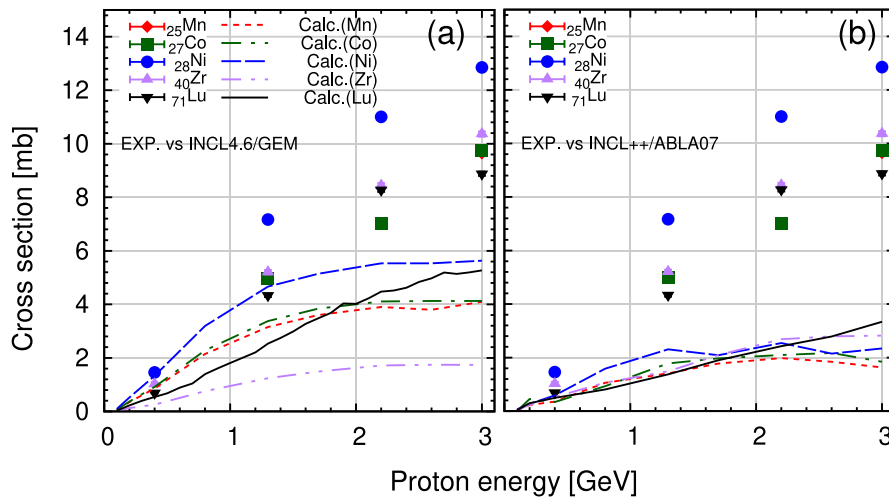
Figure 6. The ^{7}Be production cross sections for $_{25}$Mn, $_{27}$Co, $_{28}$Ni, $_{40}$Zr, and $_{71}$Lu measured at J-PARC and model predictions by INCL4.6/GEM (a) and INCL++/ABLA07 (b). The statistical uncertainties are included in the maker.

cross sections of Mn, Co, Ni, Zr, and Lu measured at J-PARC [12] were compared in Figure 6. It was found that the dependency of ^{7}Be production cross sections on the target nuclide is weak. The model calculations underestimate the experimental values as incident energy increases.

Model predictions with INCL4.6/GEM and INCL++/ABLA07 were compared with the measured data to validate their prediction powers. The INCL4.6/GEM generally reproduced the dependence of cross sections on incident proton energy, but the calculated cross sections do not necessarily agree with the experimental ones. The INCL++/ABLA07 model successfully reproduced the experimental data except for ^{7}Be production. The description of the two models should be improved to reproduce the ^{7}Be production in the future.

References

[1] Titarenko YE, Batyaev VF, Titarenko AY et al., Phys Atom. Nucl.2011;74(4):537 - 550.

[2] Michel R, Bodemann R, Busemann H et al., Nucl. Instrum. Meth. Phys. B 1997 Jan;129:153 - 193.

[3] Matsuda H, Meigo S, and Iwamoto H, J. Nucl. Sci. Technol. 2018 Apr;55(8):955 – 961.

[4] Matsuda H, Meigo S, and Iwamoto H, Maekawa F, EPJ Web Conf. 2020 239:06004.

[5] Boudard A, Cugnon J, David JC, et al. Phys Rev C. 2013 Jan;87:014606.

[6] Furihata S, Nucl. Instrum. Meth. B 2000;171:251 – 258.

[7] Mancusi D, Boudard A, Carbonell J et al., Phys. Rev. C 2015;91:034602.

[8] Kelic A, Ricciardi MV, and Schmidt KH, Proceedings of Joint ICTP-IAEA Advanced Workshop on Model Codes for Spallation Reactions, ICTP Trieste, Italy 2008;181.

[9] Meigo S, Ohi M, Kai T et al., Nucl. Instrum. Meth. Phys. B 2009:600(1):41 – 43.

[10] Sato T, Iwamoto Y, Hashimoto S et al, J. Nucl. Sci. Technol. 55(5-6), 684-690 (2018)

[11] Michel R, Dittrich B, Herpers U et al., J. Analyst 1989 Mar;114:287 – 293.

[12] Takeshita H, Meigo S, Matsuda H et al., Proceedings of J-PARC Symposium 2019 (to be published).